

---

# Compression with Bayesian Implicit Neural Representations

---

**Zongyu Guo\***

University of Science and Technology of China  
guozy@mail.ustc.edu.cn

**Gergely Flamich\***

University of Cambridge  
gf332@cam.ac.uk

**Jiajun He**

University of Cambridge  
jh2383@cam.ac.uk

**Zhibo Chen**

University of Science and Technology of China  
chenzhibo@ustc.edu.cn

**José Miguel Hernández-Lobato**

University of Cambridge  
jmh233@cam.ac.uk

## Abstract

Many common types of data can be represented as functions that map coordinates to signal values, such as pixel locations to RGB values in the case of an image. Based on this view, data can be compressed by overfitting a compact neural network to its functional representation and then encoding the network weights. However, most current solutions for this are inefficient, as quantization to low-bit precision substantially degrades the reconstruction quality. To address this issue, we propose overfitting variational Bayesian neural networks to the data and compressing an approximate posterior weight sample using relative entropy coding instead of quantizing and entropy coding it. This strategy enables direct optimization of the rate-distortion performance by minimizing the  $\beta$ -ELBO, and target different rate-distortion trade-offs for a given network architecture by adjusting  $\beta$ . Moreover, we introduce an iterative algorithm for learning prior weight distributions and employ a progressive refinement process for the variational posterior that significantly enhances performance. Experiments show that our method achieves strong performance on image and audio compression while retaining simplicity. Code is available at <https://github.com/cambridge-mlg/combiner>.

## 1 Introduction

With the celebrated development of deep learning, we have seen tremendous progress of neural data compression, particularly in the field of lossy image compression [1–4]. Taking inspiration from deep generative models, especially variational autoencoders (VAEs) [5], neural image compression models have outperformed the best manually designed image compression schemes, in terms of both objective metrics, such as PSNR and MS-SSIM [6, 7] and perceptual quality [8, 9]. However, these methods’ success is largely thanks to their elaborate architectures designed for a particular data modality. Unfortunately, this makes transferring their insights *across* data modalities challenging.

A recent line of work [10–12] proposes to solve this issue by reformulating it as a model compression problem: we treat a single datum as a continuous signal that maps coordinates to values, to which

---

\*Equal Contribution. Contact information: guozy@mail.ustc.edu.cn

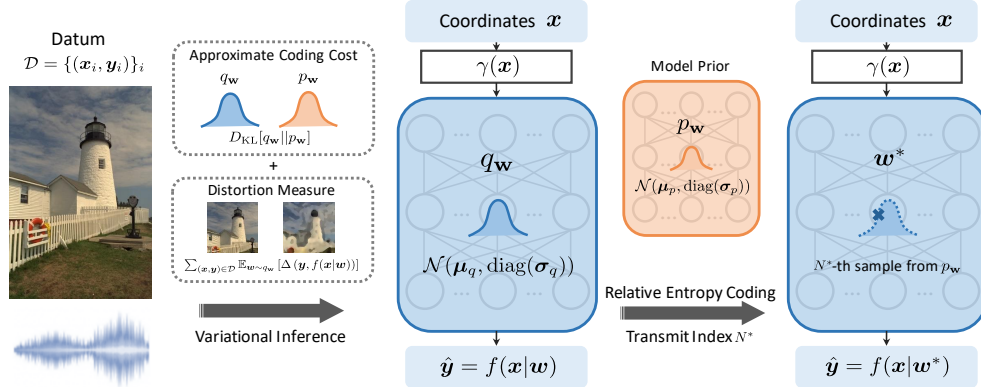


Figure 1: Framework overview of COMBINER. It first encodes a datum  $\mathcal{D}$  into Bayesian implicit neural representations, as variational posterior distribution  $q_{\mathbf{w}}$ . Then an approximate posterior sample  $\mathbf{w}^*$  is communicated from the sender to the receiver using relative entropy coding.

we overfit a small neural network called its implicit neural representation (INR). While INRs were originally proposed in [13] to study structural relationships in the data, Dupont et al. [10] have demonstrated that we can also use them for compression by encoding their weights. Since the data is conceptualised as an abstract signal, INRs allow us to develop universal, modality-agnostic neural compression methods. However, despite their flexibility, current INR-based compression methods exhibit a substantial performance gap compared to modality-specific neural compression models. This discrepancy exists because these methods cannot optimize the compression cost directly and simply quantize the parameters to a fixed precision, as opposed to VAE-based methods that rely on powerful entropy models [2, 3, 14–17] for end-to-end joint rate-distortion optimization.

In this paper, we propose a simple yet general method to resolve this issue by extending INRs to the variational Bayesian setting, i.e., we overfit a variational posterior distribution  $q_{\mathbf{w}}$  over the weights  $\mathbf{w}$  to the data, instead of a point estimate only. Then, to compress the INRs, we use a relative entropy coding (REC) algorithm [18–20] to encode a weight sample  $\mathbf{w} \sim q_{\mathbf{w}}$  from the posterior. The average coding cost of REC algorithms is approximately  $D_{\text{KL}}[q_{\mathbf{w}} \| p_{\mathbf{w}}]$ , where  $p_{\mathbf{w}}$  is the prior over the weights. Therefore, the advantage of our method is that we can directly optimize the rate-distortion trade-off of our INR by minimising its negative  $\beta$ -ELBO [21], in a similar fashion to VAE-based methods [22, 2]. We dub our method **Compression with Bayesian Implicit Neural Representations (COMBINER)**, and present a high-level description of it in Figure 1.

We propose and extensively evaluate two methodological improvements critical to enhancing COMBINER’s performance further. First, we find that a good prior distribution over the weights is crucial for good performance in practice. Thus, we derive an iterative algorithm to learn the optimal weight prior when our INRs’ variational posteriors are Gaussian. Second, adapting a technique from Havasi et al. [23], we randomly partition our weights into small blocks and compress our INRs progressively. Concretely, we encode a weight sample from one block at a time and perform a few gradient descent steps between the encoding steps to improve the posteriors over the remaining uncompressed weights. Our ablation studies show that these two techniques can contribute to more than a 4dB performance gain when compression on low-resolution images.

We evaluate COMBINER on the CIFAR-10 [24] and Kodak [25] image datasets and the LibriSpeech audio dataset [26], and show that it achieves strong performance despite being simpler than its competitors. In particular, COMBINER is not limited by the expensive meta-learning loop [27] that is present in current INR-based approaches [11, 12]. Thus we can directly optimize the INRs on an entire high-resolution image and audio file instead of splitting it into chunks. As such, our INR can capture dependencies across the entire datum, leading to significant performance gains.

To summarize, our contributions are as follows:

- We propose variational Bayesian implicit neural representations for modality-agnostic data compression by encoding INR weight samples using relative entropy coding. We call our method **Compression with Bayesian Implicit Neural Representations (COMBINER)**.

- We propose an iterative algorithm to learn a prior distribution on the weights, and a progressive strategy to refine posteriors, both of which significantly improve performance.
- We conduct experiments on the CIFAR-10, Kodak and LibriSpeech datasets, and show that COMBINER achieves strong performance despite being simpler than related methods.

## 2 Background and Motivation

In this section, we briefly review the three core ingredients of our method: implicit neural representations (INRs; [10]) and variational Bayesian neural networks (BNNs; [21]), which serve as the basis for our model of the data, and relative entropy coding, which we use to compress our model.

**Implicit neural representations:** We can conceptualise many types of data as continuous signals, such as images, audio and video. Based on neural networks’ ability to approximate any continuous function arbitrarily well [28], Stanley [13] proposed to use neural networks to represent data. In practice, this involves treating a datum  $\mathcal{D}$  as a point set, in which each data point corresponds to a coordinate-signal value pair  $(\mathbf{x}, \mathbf{y})$ , and overfitting a small neural network  $f(\mathbf{x} \mid \mathbf{w})$ , usually a multilayer perceptron (MLP) parameterised by weights  $\mathbf{w}$ , which is then called the *implicit neural representation* (INR) of  $\mathcal{D}$ . Recently, Dupont et al. [10] popularised INRs for lossy data compression by noting that compressing the INR’s weights  $\mathbf{w}$  amounts to compressing  $\mathcal{D}$ . However, their method has a crucial shortcoming: they assume a uniform coding distribution over  $\mathbf{w}$ , leading to a constant *rate*, and overfit the INR only using the *distortion* as the loss. Thus, unfortunately, they can only control the compression cost by varying the number of weights since they show that quantizing the weights to low precision significantly degrades performance. In this paper, we solve this issue using variational Bayesian neural networks, which we discuss next.

**Variational Bayesian neural networks:** Based on the minimum description length principle, we can explicitly control the network weights’ compression cost by making them stochastic. Concretely, we introduce a *prior*  $p(\mathbf{w})$  (abbreviated as  $p_{\mathbf{w}}$ ) and a *variational posterior*  $q(\mathbf{w} \mid \mathcal{D})$  (abbreviated as  $q_{\mathbf{w}}$ ) over the weights, in which case their information content is given by the *Kullback-Leibler (KL) divergence*  $D_{\text{KL}}[q_{\mathbf{w}} \parallel p_{\mathbf{w}}]$ , as shown in [29]. Therefore, for distortion measure  $\Delta$  and a coding budget of  $C$  bits, we can optimize the constrained objective

$$\min_{q_{\mathbf{w}}} \sum_{(\mathbf{x}, \mathbf{y}) \in \mathcal{D}} \mathbb{E}_{\mathbf{w} \sim q_{\mathbf{w}}} [\Delta(\mathbf{y}, f(\mathbf{x} \mid \mathbf{w}))], \quad \text{subject to } D_{\text{KL}}[q_{\mathbf{w}} \parallel p_{\mathbf{w}}] \leq C. \quad (1)$$

In practice, we introduce a slack variable  $\beta$  and optimize the Lagrangian dual, which yields:

$$\mathcal{L}_{\beta}(\mathcal{D}, q_{\mathbf{w}}, p_{\mathbf{w}}) = \sum_{(\mathbf{x}, \mathbf{y}) \in \mathcal{D}} \mathbb{E}_{\mathbf{w} \sim q_{\mathbf{w}}} [\Delta(\mathbf{y}, f(\mathbf{x} \mid \mathbf{w}))] + \beta \cdot D_{\text{KL}}[q_{\mathbf{w}} \parallel p_{\mathbf{w}}] + \text{const.}, \quad (2)$$

with different settings of  $\beta$  corresponding to different coding budgets  $C$ . Thus, optimizing  $\mathcal{L}_{\beta}(\mathcal{D}, q_{\mathbf{w}}, p_{\mathbf{w}})$  is equivalent to directly optimizing the rate-distortion trade-off for a given rate  $C$ .

**Relative entropy coding with A\* coding:** We will use *relative entropy coding* to directly encode a *single random weight sample*  $\mathbf{w} \sim q_{\mathbf{w}}$  instead of quantizing a point estimate and entropy coding it. This idea was first proposed by Havasi et al. [23] for model compression, who introduced minimal random coding (MRC) to encode a weight sample. In our paper, we use *depth-limited, global-bound A\* coding* instead, to which we refer as A\* coding hereafter for brevity’s sake [30, 20]. We present it in Appendix A for completeness. A\* coding is an importance sampling algorithm that draws<sup>2</sup>  $N = \lceil 2^{D_{\text{KL}}[q_{\mathbf{w}} \parallel p_{\mathbf{w}}] + t} \rceil$  independent samples  $\mathbf{w}_1, \dots, \mathbf{w}_N$  from the prior  $p_{\mathbf{w}}$  for some parameter  $t \geq 0$ , and computes their importance weights  $r_i = \log(q_{\mathbf{w}}(\mathbf{w}_i)/p_{\mathbf{w}}(\mathbf{w}_i))$ . Then, in a similar fashion to the Gumbel-max trick [32], it randomly perturbs the importance weights and selects the sample with the greatest perturbed weight. Unfortunately, this procedure returns an approximate sample with distribution  $\tilde{q}_{\mathbf{w}}$ . However, Theis and Yosri [33] have shown that the total variation distance  $\|q_{\mathbf{w}} - \tilde{q}_{\mathbf{w}}\|_{\text{TV}}$  vanishes exponentially quickly as  $t \rightarrow \infty$ . Thus,  $t$  can be thought of as a free parameter of the algorithm that trades off compression rate for sample quality. Furthermore, A\* coding is more efficient than MRC [23] in the following sense: Let  $N_{\text{MRC}}$  and  $N_{\text{A}^*}$  be the codes returned by MRC and A\* coding, respectively, when given the same target and proposal distribution as input. Then,  $\mathbb{H}[N_{\text{A}^*}] \leq \mathbb{H}[N_{\text{MRC}}]$ , hence using A\* coding is always strictly more efficient [33].

<sup>2</sup>In practice, we use quasi-random number generation with multi-dimensional Sobol sequences [31] to simulate our random variables to ensure that they cover the sample space as evenly as possible.

---

**Algorithm 1** Learning the model prior

---

**Require:** Training data  $\{\mathcal{D}_i\} = \{\mathcal{D}_1, \mathcal{D}_2, \dots, \mathcal{D}_M\}$ .

**Initialize :** The model posteriors  $q_{\mathbf{w}}^{(i)} = \mathcal{N}(\boldsymbol{\mu}_i, \text{diag}(\boldsymbol{\sigma}_i))$  of every training datum  $\mathcal{D}_i$ .

**Initialize :** The model priors  $p_{\mathbf{w};\boldsymbol{\theta}_p} = \mathcal{N}(\boldsymbol{\mu}_p, \text{diag}(\boldsymbol{\sigma}_p))$ .

**repeat until convergence**

**for**  $i \leftarrow 1$  to  $M$  **do**

$\{q_{\mathbf{w}}^{(i)}\} \leftarrow \arg \min_{\{q_{\mathbf{w}}^{(i)}\}} \mathcal{L}(\boldsymbol{\theta}_p, \{q_{\mathbf{w}}^{(i)}\})$        $\triangleright$  Gradient descent for optimizing posteriors

**end for**

$\boldsymbol{\theta}_p \leftarrow \arg \min_{\boldsymbol{\theta}_p} \mathcal{L}(\boldsymbol{\theta}_p, \{q_{\mathbf{w}}^{(i)}\})$        $\triangleright$  Closed-form solution in Equation (5)

**end repeat**

**Return**  $p_{\mathbf{w};\boldsymbol{\theta}_p} = \mathcal{N}(\boldsymbol{\mu}_p, \text{diag}(\boldsymbol{\sigma}_p))$

---

### 3 Compression with Bayesian Implicit Neural Representations

We now introduce our method, dubbed **Compression with Bayesian Implicit Neural Representations** (COMBINER). It extends INRs to the variational Bayesian setting by introducing a variational posterior  $q_{\mathbf{w}}$  over the network weights and fits INRs to the data  $\mathcal{D}$  by minimizing Equation (2). Since encoding the model weights is equivalent to compressing the data  $\mathcal{D}$ , Equation (2) corresponds to jointly optimizing a given rate-distortion trade-off for the data. This is the main advantage of the proposed COMBINER, unlike other INR-based compression methods that optimize the distortion only and cannot optimize jointly with the accurate coding cost. Moreover, another important difference is that we encode a random weight sample  $\mathbf{w} \sim q_{\mathbf{w}}$  from the weight posterior using A\* coding [20] instead of quantizing the weights and entropy coding them. At a high level, COMBINER applies the model compression approach proposed by Havasi et al. [23] to encode variational Bayesian INRs, albeit with significant improvements which we discuss in Sections 3.1 and 3.2.

In this paper, we only consider networks with a diagonal Gaussian prior  $p_{\mathbf{w}} = \mathcal{N}(\boldsymbol{\mu}_p, \text{diag}(\boldsymbol{\sigma}_p))$  and posterior  $q_{\mathbf{w}} = \mathcal{N}(\boldsymbol{\mu}_q, \text{diag}(\boldsymbol{\sigma}_q))$  for mean and variance vectors  $\boldsymbol{\mu}_p, \boldsymbol{\mu}_q, \boldsymbol{\sigma}_p, \boldsymbol{\sigma}_q$ . Here,  $\text{diag}(\mathbf{v})$  denotes a diagonal matrix with  $\mathbf{v}$  on the main diagonal. Following Havasi et al. [23], we optimize the variational parameters  $\boldsymbol{\mu}_q$  and  $\boldsymbol{\sigma}_q$  using the local reparameterization trick [34] and, in Section 3.1, we derive an iterative algorithm to learn the prior parameters  $\boldsymbol{\mu}_p$  and  $\boldsymbol{\sigma}_p$ .

#### 3.1 Learning the Model Prior on the Training Set

To guarantee that COMBINER performs well in practice, it is critical that we find a good prior  $p_{\mathbf{w}}$  over the network weights, since it serves as the proposal distribution for A\* coding and thus directly impacts the method’s coding efficiency. Naturally, however, different network parameters exhibit varying importance when representing distinct data. Consequently, learning *parameter-wise* model priors is beneficial, as it enables the effective allocation of bits to different network parameters.

To this end, we provide an iterative algorithm to learn the model priors, described in Algorithm 1. Based on a set of training data  $\{\mathcal{D}_i\} = \{\mathcal{D}_1, \mathcal{D}_2, \dots, \mathcal{D}_M\}$ , we aim to find the prior parameters  $\boldsymbol{\theta}_p = \{\boldsymbol{\mu}_p, \boldsymbol{\sigma}_p\}$  which minimize the average rate-distortion objective across all training instances:

$$\bar{\mathcal{L}}_{\beta}(\boldsymbol{\theta}_p, \{q_{\mathbf{w}}^{(i)}\}) = \frac{1}{M} \sum_{i=1}^M \mathcal{L}_{\beta}(\mathcal{D}_i, q_{\mathbf{w}}^{(i)}, p_{\mathbf{w};\boldsymbol{\theta}_p}). \quad (3)$$

In Equation (3) we write  $q_{\mathbf{w}}^{(i)} = \mathcal{N}(\boldsymbol{\mu}_q^{(i)}, \text{diag}(\boldsymbol{\sigma}_q^{(i)}))$ , and  $p_{\mathbf{w};\boldsymbol{\theta}_p} = \mathcal{N}(\boldsymbol{\mu}_p, \text{diag}(\boldsymbol{\sigma}_p))$  that explicitly notes the prior’s dependence on its parameters. Now, we propose a coordinate descent algorithm to minimize the objective in Equation (3), shown in Algorithm 1. To begin, we randomly initialize the model prior and the posteriors, and alternate the following two steps to optimize  $\{q_{\mathbf{w}}^{(i)}\}$  and  $\boldsymbol{\theta}_p$ :

1. **Optimize the variational posteriors:** We fix the prior parameters  $\boldsymbol{\theta}_p$  and optimize the posteriors using the local reparameterization trick [35] with gradient descent. Note that, given  $\boldsymbol{\theta}_p$ , optimizing  $\bar{\mathcal{L}}_{\beta}(\boldsymbol{\theta}_p, \{q_{\mathbf{w}}^{(i)}\})$  can be split into  $M$  independent optimization prob-

lems, which we can perform in parallel:

$$\text{for each } i = 1, \dots, M: \quad q_{\mathbf{w}}^{(i)} = \arg \min_q \mathcal{L}_\beta(\mathcal{D}_i, q, p_{\mathbf{w}}; \theta_p). \quad (4)$$

2. **Updating prior:** We fix the posteriors  $\{q_{\mathbf{w}}^{(i)}\}$  and update the model prior by computing  $\theta_p = \arg \min_{\theta} \bar{\mathcal{L}}_\beta(\theta_p, \{q_{\mathbf{w}}^{(i)}\})$ . In the Gaussian case, this admits a closed-form solution:

$$\boldsymbol{\mu}_p = \frac{1}{M} \sum_{i=1}^M \boldsymbol{\mu}_q^{(i)}, \quad \boldsymbol{\sigma}_p = \frac{1}{M} \sum_{i=1}^M [\boldsymbol{\sigma}_q^{(i)} + (\boldsymbol{\mu}_q^{(i)} - \boldsymbol{\mu}_p)^2]. \quad (5)$$

We provide the full derivation of this procedure in Appendix B. Note that by the definition of coordinate descent, the value of  $\bar{\mathcal{L}}_\beta(\theta_p, \{q_{\mathbf{w}}^{(i)}\})$  decreases after each iteration, which ensures that our estimate of  $\theta_p$  converges to some optimum.

### 3.2 Compression with Posterior Refinement

Algorithm 1 provides an efficient solution for learning a parameter-wise model prior using a few training samples. Once the model prior is obtained, it can be used by the sender to train the variational posterior distribution for a specific test datum, as illustrated by Equation (2). To further improve the performance of INR compression, we also adopt a progressive posterior refinement strategy, a concept originally proposed in [23] for Bayesian model compression.

To motivate this strategy, we first consider the *optimal weight posterior*  $q_{\mathbf{w}}^*$ . Fixing the data  $\mathcal{D}$ , trade-off parameter  $\beta$  and weight prior  $p_{\mathbf{w}}$ ,  $q_{\mathbf{w}}^*$  is given by  $q_{\mathbf{w}}^* = \arg \min_q \mathcal{L}_\beta(\mathcal{D}, q, p_{\mathbf{w}})$ , where the minimization is performed over the set of all possible target distributions  $q$ . To compress  $\mathcal{D}$  using our Bayesian INR, ideally we would like to encode a sample  $\mathbf{w}^* \sim q_{\mathbf{w}}^*$ , as it achieves optimal performance on average by definition. Unfortunately, finding  $q_{\mathbf{w}}^*$  is intractable in general, hence we restrict the search over the set of all factorized Gaussian distributions in practice, which yields a rather crude approximation. However, note that for compression, we only care about encoding a **single, good quality sample** using relative entropy coding. To achieve this, Havasi et al. [23] suggest partitioning the weight vector  $\mathbf{w}$  into  $K$  blocks  $\mathbf{w}_{1:K} = \{\mathbf{w}_1, \dots, \mathbf{w}_K\}$ . For example, we might partition the weights per MLP layer with  $\mathbf{w}_i$  representing the weights on layer  $i$ , or into a preset number of random blocks; at the extremes, we could partition  $\mathbf{w}$  per dimension, or we could just set  $K = 1$  for the trivial partition. Now, to obtain a good quality posterior sample given a partition  $\mathbf{w}_{1:K}$ , we start with our crude posterior approximation and obtain

$$q_{\mathbf{w}} = q_{\mathbf{w}_1} \times \dots \times q_{\mathbf{w}_K} = \arg \min_{q_1, \dots, q_K} \mathcal{L}_\beta(\mathcal{D}, q_1 \times \dots \times q_K, p_{\mathbf{w}}), \quad (6)$$

where each of the  $K$  minimization procedures takes place over the appropriate family of factorized Gaussian distributions. Then, we draw a sample  $\mathbf{w}_1 \sim q_{\mathbf{w}_1}$  and *refine* the remaining approximation:

$$q_{\mathbf{w}|\mathbf{w}_1} = q_{\mathbf{w}_2|\mathbf{w}_1} \times \dots \times q_{\mathbf{w}_K|\mathbf{w}_1} = \arg \min_{q_2, \dots, q_K} \mathcal{L}_\beta(\mathcal{D}, q_2 \times \dots \times q_K, p_{\mathbf{w}} | \mathbf{w}_1), \quad (7)$$

where  $\mathcal{L}_\beta(\cdot | \mathbf{w}_1)$  indicates that  $\mathbf{w}_1$  is fixed during the optimization. We now draw  $\mathbf{w}_2 \sim q_{\mathbf{w}_2|\mathbf{w}_1}$  to obtain the second chunk of our final sample. In total, we iterate the refinement procedure  $K$  times, progressively conditioning on more blocks, until we obtain our final sample  $\mathbf{w} = \mathbf{w}_{1:K}$ . Note that already after the first step, the approximation becomes *conditionally factorized Gaussian*, which makes it far more flexible, and thus it approximates  $q_{\mathbf{w}}^*$  much better [18].

**Combining the refinement procedure with compression:** Above, we assumed that after each refinement step  $k$ , we draw the next weight block  $\mathbf{w}_k \sim q_{\mathbf{w}_k|\mathbf{w}_{1:k-1}}$ . However, as suggested in [23], we can also extend the scheme to incorporate relative entropy coding, by encoding an approximate sample  $\tilde{\mathbf{w}}_k \sim \tilde{q}_{\mathbf{w}_k|\tilde{\mathbf{w}}_{1:k-1}}$  with A\* coding instead. This way, we actually feed two birds with one stone: the refinement process allows us to obtain a better overall approximate sample  $\tilde{\mathbf{w}}$  by extending the variational family and by correcting for the occasional bad quality chunk  $\tilde{\mathbf{w}}_k$  at the same time, thus making COMBINER more robust in practice.

### 3.3 COMBINER in Practice

Given a partition  $\mathbf{w}_{1:K}$  of the weight vector  $\mathbf{w}$ , we use A\* coding to encode a sample  $\tilde{\mathbf{w}}_k$  from each block. Let  $\delta_k = D_{\text{KL}}[q_{\mathbf{w}_k|\tilde{\mathbf{w}}_{1:k-1}} \| p_{\mathbf{w}_k}]$  represent the KL divergence in block  $k$  after the completion

of the first  $k - 1$  refinement steps, where we have already simulated and encoded samples from the first  $k - 1$  block. As we discussed in Section 2, we need to simulate  $\lceil 2^{\delta_k+t} \rceil$  samples from the prior  $p_{\mathbf{w}_k}$  to ensure that the sample  $\tilde{\mathbf{w}}_k$  encoded by A\* coding has low bias. Therefore, for our method to be computationally tractable, it is important to ensure that there is no block with large divergence  $\delta_k$ . In fact, to guarantee that COMBINER’s runtime is consistent, we would like the divergences across all blocks to be approximately equal, i.e.,  $\delta_i \approx \delta_j$  for  $0 \leq i, j \leq K$ . To this end, we set a bit-budget of  $\kappa$  bits per block and below we describe the techniques we used to ensure  $\delta_k \approx \kappa$  for all  $k = 1, \dots, K$ . Unless stated otherwise, we set  $\kappa = 16$  bits and  $t = 0$  in our experiments.

First, we describe how we partition the weight vector based on the training data, to approximately enforce our budget on average. Note that we control COMBINER’s rate-distortion trade-off by varying  $\beta$  in its training loss in Equation (3). Thus, when we run Algorithm 1 to learn the prior, we also estimate the expected coding cost of the data given  $\beta$  as  $c_\beta = \frac{1}{M} \sum_{i=1}^M D_{\text{KL}}[q_{\mathbf{w}}^{(i)} \| p_{\mathbf{w}}]$ . Then, we set the number of blocks as  $K_{\beta, \kappa} = \lceil c_\beta / \kappa \rceil$  and we partition the weight vector such that the average divergence  $\bar{\delta}_k$  of each block estimated on the training data matches the coding budget, i.e.,  $\bar{\delta}_k \approx \kappa$  bits. Unfortunately, allocating individual weights to the blocks under this constraint is equivalent to the NP-hard bin packing problem [36]. However, we found that randomly permuting the weights and greedily assigning them using the next-fit bin packing algorithm [37] worked well in practice.

**Relative entropy coding-aware finetuning:** Assume we now wish to compress some data  $\mathcal{D}$ , and we already selected the desired rate-distortion trade-off  $\beta$ , ran the prior learning procedure, fixed a bit budget  $\kappa$  for each block and partitioned the weight vector using the procedure from the previous paragraph. Despite our effort to set the blocks so that the average divergence  $\bar{\delta}_k \approx \kappa$  in each block on the training data, if we optimized the variational posterior  $q_{\mathbf{w}}$  using  $\mathcal{L}_\beta(\mathcal{D}, q_{\mathbf{w}}, p_{\mathbf{w}})$ , it is unlikely that the actual divergences  $\delta_k$  would match  $\kappa$  in each block. Therefore, we adapt the optimization procedure from [23], and we use a modified objective for each of the  $k$  posterior refinement steps:

$$\mathcal{L}_{\lambda_{k:K}}(\mathcal{D}, q_{\mathbf{w}|\tilde{\mathbf{w}}_{1:k-1}}, p_{\mathbf{w}}) = \sum_{(\mathbf{x}, \mathbf{y}) \in \mathcal{D}} \mathbb{E}_{\mathbf{w} \sim q_{\mathbf{w}}} [\Delta(\mathbf{y}, f(\mathbf{x} | \mathbf{w}))] + \sum_{i=k}^K \lambda_i \cdot \delta_i, \quad (8)$$

where  $\lambda_{k:K} = \{\lambda_k, \dots, \lambda_K\}$  are slack variables, which we dynamically adjust during optimization. Roughly speaking, at each optimization step, we compute each  $\delta_i$  and increase its penalty term  $\lambda_i$  if it exceeds the coding budget (i.e.,  $\delta_i > \kappa$ ) and decrease the penalty term otherwise. See Appendix C for the detailed algorithm.

**The comprehensive COMBINER pipeline:** We now provide a brief summary of the entire COMBINER compression pipeline. To begin, given a dataset  $\{\mathcal{D}_1, \dots, \mathcal{D}_M\}$ , we select an appropriate INR architecture, and run the prior learning procedure (Algorithm 1) with different settings for  $\beta$  to obtain priors for a range of rate-distortion trade-offs.

To compress a new data point  $\mathcal{D}$ , we select a prior with the desired rate-distortion trade-off and pick a blockwise coding budget  $\kappa$ . Then, we partition the weight vector  $\mathbf{w}$  based on  $\kappa$ , and finally, we run the relative entropy coding-aware finetuning procedure from above, using A\* coding to compress the weight blocks between the refinement steps to obtain the compressed representation of  $\mathcal{D}$ .

## 4 Related Work

**Neural Compression.** Despite their short history, neural image compression methods’ rate-distortion performance rapidly surpassed traditional image compression standards [16, 7, 9]. The current state-of-the-art methods follow a variational autoencoder framework [2], optimizing the rate-distortion loss jointly. To estimate the rate of the quantized latent variables, many prior works [2, 3, 14–17] are dedicated to improving the entropy model. Such VAE-based compression framework has been extended to other data modalities, e.g., video [38] or point cloud compression [39]. Mainstream methods quantize the latent variables produced by the encoder for transmission. Since the gradient of quantization is zero almost everywhere, it makes the standard back-propagation inapplicable [40]. A popular solution [22] is to use additive uniform noise during training to approximate the quantization error, but it suffers from a train-test mismatch [41]. Relative entropy coding (REC) algorithms [19] eliminate this mismatch, as they can directly encode samples from the VAEs’ latent posterior. Moreover, they bring unique advantages to compression with additional constraints, such as lossy compression with realism constraints [42, 43] and differentially private compression [44].

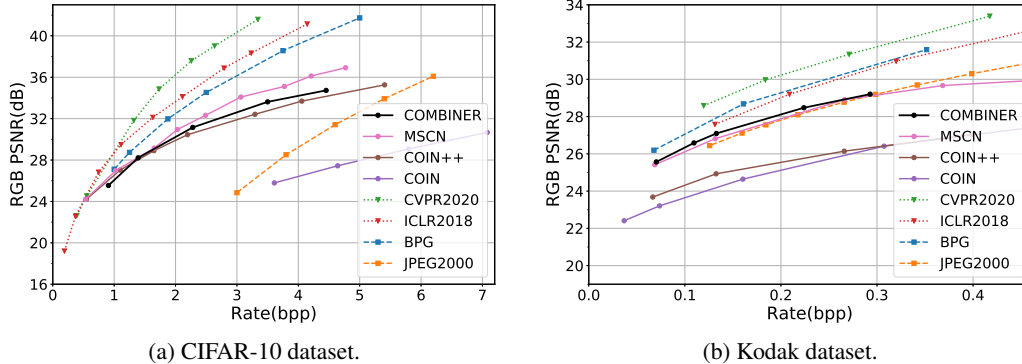


Figure 2: Rate-distortion curves on two image datasets. In both figures, **solid lines** denote INR-based methods, **dotted lines** denote VAE-based methods and **dashed lines** denote classical methods. Examples of decoded Kodak images are provided in Appendix E.4.

**Compressing with INRs.** INRs are parametric functional representations of data that offer many benefits over conventional grid-based representations, such as compactness and memory-efficiency [45–47]. Compression with INRs has emerged as a new paradigm for neural compression [10], effective in compressing images [48], climate data [11], videos [49] and 3D scenes [50]. Usually, obtaining the INRs involves overfitting a neural network to a new signal, which is computationally costly [51]. Therefore, to ease the computational burden, some works [11, 48, 12] employ meta-learning loops [27] that largely reduce the fitting times during encoding. However, due to the expensive nature of the meta-learning process, these methods need to crop the data into patches to make training with second-order gradients practical. The biggest difficulty the current INR-based methods face is that quantizing the INR weights and activations can significantly degrade their performance, due to the brittle nature of the heavily overfitted parameters. Our method solves this issue by fitting a variational posterior over the parameters, from which we can encode samples directly using REC, eliminating the mismatch caused by quantization. Concurrent to our work, Schwarz et al. [52] introduced a method to learn a better coding distribution for the INR weights using a VAE, in a similar vein to our prior learning method in Algorithm 1. Their method achieves impressive performance on image and audio compression tasks, but is significantly more complex than our method: they run an expensive meta-learning procedure to learn the backbone architecture for their INRs and train a VAE to encode the INRs, making the already long training phase even longer.

## 5 Experiments

Our proposed method, Compression with Bayesian INRs (COMBINER), offers a simple and natural solution for joint rate-distortion optimization of INRs. In this paper, we conduct experiments predominantly for image compression on both the low-resolution CIFAR-10 dataset [24] and the high-resolution Kodak dataset [25]. A detailed analysis of the proposed approach is presented in Section 5.2, where we demonstrate its ability to adaptively activate or prune the INR parameters, leading to more efficient compression of specific signals. We also show its strong performance for audio compression, as a more comprehensive evaluation in different data modalities.

### 5.1 Image Compression

**Datasets.** Experiments for image compression were conducted on both the CIFAR-10 dataset [24] and the Kodak dataset [25]. For the CIFAR-10 dataset, which contains images of  $32 \times 32$  pixels, we randomly selected 2048 images from the training set for learning the model prior, and evaluated our model on all 10,000 images in the test set. Another group of experiments was conducted on the Kodak dataset, a commonly used benchmark for image compression that contains 24 images with resolutions of either  $768 \times 512$  or  $512 \times 768$ . To learn the model prior, we randomly cropped 512 patches from the CLIC training set [53], each with the same resolution of Kodak images.

**Models.** Following previous methods [10–12], we utilize SIREN [45] as the network architecture. Input coordinates  $\mathbf{x}$  are transformed into Fourier embeddings [46] before being fed into the MLP network, depicted as  $\gamma(\mathbf{x})$  in Figure 1. For the model structure, we experimentally find a 4-layer

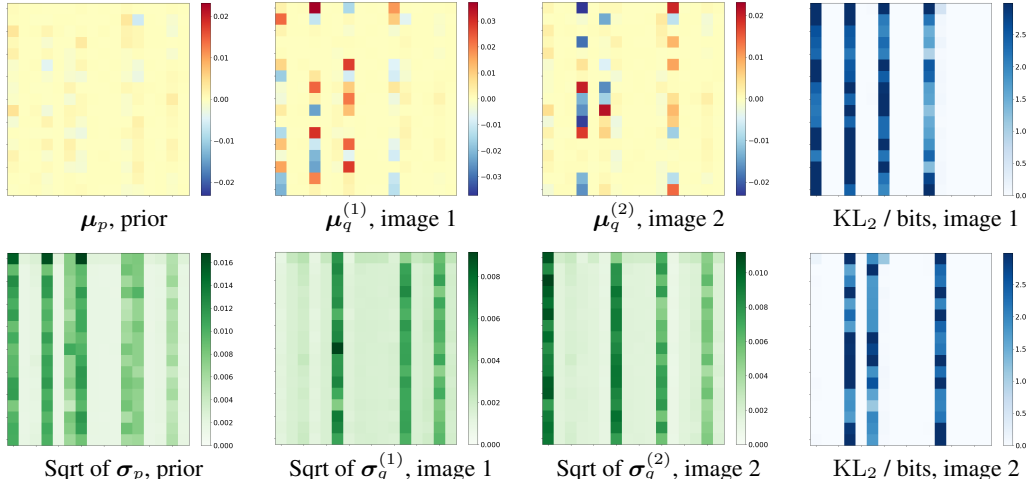


Figure 3: Visualizations on the variational posteriors and prior. We focus on a specific layer with 16 hidden units. Therefore, each visualization map has 16 columns representing 16 hidden units. Each map is in the shape of  $17 \times 16$  because weight and bias are concatenated (the last row is bias). Note we are visualizing the square root (as “sqrt” here) of variance  $\sigma$ , i.e., the standard deviation.

MLP with 16 hidden units per layer and 32 Fourier embeddings works well on CIFAR-10. When training on the CLIC set and testing on the Kodak dataset, we use two models in different sizes to cover multiple rate points. The detailed model structure and other experimental settings can be found in Appendix D. It is noteworthy that the networks utilized in our experiments are quite small. The model used for compressing images on CIFAR-10 contains only 1,123 parameters, and even the larger model for compressing high-resolution Kodak images contains merely 21,563 parameters.

**Performance.** We benchmark our method against classical codecs including JPEG2000 and BPG, and INR-based codecs including COIN [10], COIN++ [11], and MSCN [12]. Additionally, we include results from VAE-based codecs such as ICLR2018 [2] and CVPR2020 [4] for reference. Their rate-distortion performances are compared in Figure 2. We can observe that COMBINER exhibits competitive performance on the CIFAR-10 dataset, on par with COIN++ and marginally lower than MSCN. However, our proposed COMBINER presents impressive performance on the Kodak dataset, surpassing JPEG2000 and other INR-based codecs. This superior performance can be attributed to the fact that our method does not necessitate the computation of second-order gradients during training. Then the whole high-resolution image can be compressed using a single MLP network, which facilitates the model to capture the global redundancies of images.

## 5.2 Analysis and Ablation Study

**Model Visualizations.** For a better understanding of our method, we further provide some visualizations. Specifically, we investigate on a model trained on the CIFAR-10 dataset with  $\beta = 10^{-6}$ . This MLP model is built with four layers and 16 hidden units in the intermediate layers. Here we take the second layer for visualization. Note that we use the theoretical KL value as an approximate to the coding cost, which means in this section of visualizations, we do not conduct practical relative entropy coding or progressive finetuning of the posterior groups.

As shown in Figure 3, we first visualize the learned model prior (both  $\mu_p$  and  $\sigma_p$ ) in the left column. We then display the variational posteriors of two distinct images in the second and third columns. The KL divergence  $D_{\text{KL}}[q_w \| p_w]_2$  is visualized in the rightmost column. Since this layer incorporates 16 hidden units, the weight matrix of parameters has a  $17 \times 16$  shape, where weights and bias are concatenated (the bias is represented by the last row). Interestingly, there are seven green columns within  $\sigma_p$ , indicating that only seven hidden units of this layer would be activated for signal representation at this specific rate point. For instance, when representing image 1 that is randomly selected from the CIFAR-10 test set, four columns are activated for representation. This activation is evident in the four blue columns within the KL map, which require a few bits to transmit the sample of the posterior distribution. Likewise, three hidden units are engaged in the representation of image 2. As their variational Gaussian distributions exhibit a unimodal peak with almost zero variance, the

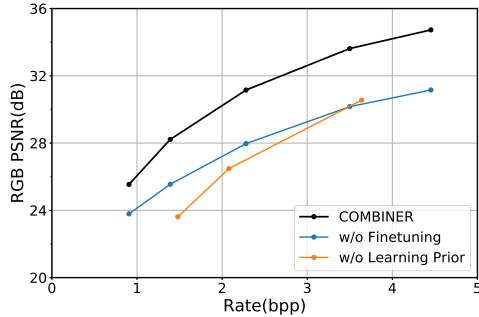


Figure 4: Ablation study on CIFAR-10.

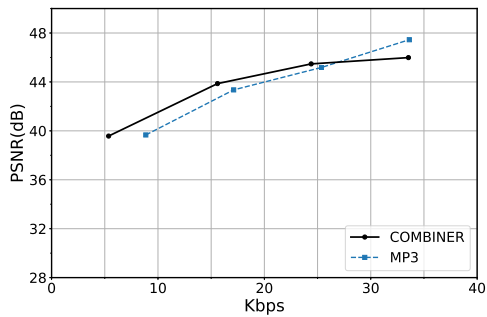


Figure 5: Performance of compressing audios.

posterior distributions at these activated columns basically approach a Dirac delta distribution. In summary, by optimizing the rate-distortion objective, our proposed method can adaptively activate or prune network parameters to represent a specific signal.

**Ablation Study.** Ablation studies are conducted on the CIFAR-10 dataset to verify the effectiveness of learning the model prior iteratively and finetuning the posteriors progressively. For the first ablation study, we do not learn model priors with the iterative algorithm and instead transmit layer-wise priors, similar to [23]. For the second ablation study, we directly compress approximate samples from the overfitted posterior distributions after partitioning them into groups. Each group is compressed with 16 bits and we do not finetune the posterior groups sequentially. As shown in Figure 4, it can be observed that both of these two techniques bring significant gains. In particular, progressively finetuning the posteriors is more effective at high bitrate points, and learning model priors increase the performance stably with a 4dB gain.

**Analysis of Complexity.** Similar to COIN [10], the encoding period in our method takes thousands of iterations to learn the variational posterior distributions of Bayesian INR. Our method also spends additional thousands of iterations to progressively finetune the posterior. However, our decoding process is remarkably fast, matching the speed of the original COIN. See Appendix E.1 for the specific coding time. While our main contribution is this novel compression approach, we have not specifically tried to reduce encoding time complexity in this paper. Furthermore, regarding the training time, our approach does not involve computing second-order gradients, and only requires a small training set. We show in Appendix E.2 that the model prior of Kodak dataset can be learned from only 32 training data. Therefore, COMBINER retains simplicity compared with COIN++ [11] and other methods that rely on meta-learning loops.

### 5.3 Compressing Data in Other Modalities

To demonstrate the effectiveness of COMBINER for compressing data in other modalities, we also conduct experiments on audio data. Since our method does not need to compute the second-order gradient during training, we can directly compress a long audio segment with a single INR model. We evaluate our method on LibriSpeech [26], a speech dataset recorded at a 16kHz sampling rate. We train the model prior with 3-second audios, i.e., 48000 samples in a single chunk. The detailed experimental setup is described in Appendix D. Due to the time-consuming encoding process of COMBINER, we restrict our evaluation to 24 randomly selected audio chunks from test set. Since we lack COIN++ statistics for this subset of 24 audio chunks, we only compare our method with the classical coding method MP3 (implemented with ffmpeg package), which has been shown to be much better than COIN++ on the complete test set [11]. Figure 5 shows our method can outperforms MP3 at low bitrate points, which verifies the effectiveness of our method on compressing audios. Moreover, we also conducted another group of experiments where the audios are cropped into shorter chunks, which is shown in the Appendix E.3.

## 6 Conclusion and Limitations

**Conclusion.** In this paper, we propose COMBINER, a new neural compression approach that first encodes data as variational Bayesian implicit neural representations, and then communicates an approximate posterior weight sample using relative entropy coding. Unlike previous INR-based neural

codecs, COMBINER supports joint rate-distortion optimization and thus is able to adaptively activate and prune the network parameters. Revolving around this framework, we also introduce an iterative algorithm for learning prior weight distributions and refine the variational posterior progressively that significantly enhances the rate-distortion performance. Experiments demonstrate our strong compression performance on low-resolution and high-resolution images and audios, showcasing the great potential of compression with variational Bayesian implicit neural representations.

**Limitations.** Several limitations exist in our proposed new compression method. First, as discussed in Section 5.2, while the decoding process of COMBINER is fast, its encoding time is considerably longer. Optimizing the variational posterior distributions requires thousands of iterations, and progressively fine-tuning them is also time-consuming. Probabilistic MAML [54] could potentially reduce the encoding time, but it may lead to a more complex training process. Second, Bayesian neural networks are inherently sensitive to initialization [55]. It can sometimes require considerable effort to identify the optimal initialization setting for achieving both training stability and superior rate-distortion performance. Despite these challenges, we believe COMBINER paves the path for joint rate-distortion optimization of compression with INRs.

## 7 Acknowledgement

ZG acknowledges funding from the Outstanding PhD Student Program at the University of Science and Technology of China. ZC is supported in part by National Natural Science Foundation of China under Grant U1908209, 62021001. GF acknowledges funding from DeepMind.

## References

- [1] Lucas Theis, Wenzhe Shi, Andrew Cunningham, and Ferenc Huszár. Lossy image compression with compressive autoencoders. In *5th International Conference on Learning Representations, ICLR 2017*, 2017. 1
- [2] Johannes Ballé, David Minnen, Saurabh Singh, Sung Jin Hwang, and Nick Johnston. Variational image compression with a scale hyperprior. In *6th International Conference on Learning Representations, ICLR 2018*, 2018. 2, 6, 8
- [3] David Minnen, Johannes Ballé, and George Toderici. Joint autoregressive and hierarchical priors for learned image compression. In *Advances in Neural Information Processing Systems*, pages 10794–10803, 2018. 2, 6
- [4] Zhengxue Cheng, Heming Sun, Masaru Takeuchi, and Jiro Katto. Learned image compression with discretized gaussian mixture likelihoods and attention modules. In *Proceedings of the IEEE/CVF Conference on Computer Vision and Pattern Recognition*, pages 7939–7948, 2020. 1, 8
- [5] Diederik P. Kingma and Max Welling. In *2th International Conference on Learning Representations, ICLR 2014*, 2014. 1
- [6] Dailan He, Ziming Yang, Weikun Peng, Rui Ma, Hongwei Qin, and Yan Wang. ELIC: efficient learned image compression with unevenly grouped space-channel contextual adaptive coding. In *Proceedings of the IEEE/CVF Conference on Computer Vision and Pattern Recognition*, pages 5718–5727, 2022. 1
- [7] Jinming Liu, Heming Sun, and Jiro Katto. Learned image compression with mixed transformer-cnn architectures. *arXiv preprint arXiv:2303.14978*, 2023. 1, 6
- [8] Eirikur Agustsson, Michael Tschannen, Fabian Mentzer, Radu Timofte, and Luc Van Gool. Generative adversarial networks for extreme learned image compression. In *Proceedings of the IEEE/CVF International Conference on Computer Vision*, pages 221–231, 2019. 1
- [9] Fabian Mentzer, George Toderici, Michael Tschannen, and Eirikur Agustsson. High-fidelity generative image compression. In *Advances in Neural Information Processing Systems*, volume 33, pages 11913–11924, 2020. 1, 6
- [10] Emilien Dupont, Adam Golinski, Milad Alizadeh, Yee Whye Teh, and Arnaud Doucet. COIN: compression with implicit neural representations. *arXiv preprint arXiv:2103.03123*, 2021. 1, 2, 3, 7, 8, 9, 18

- [11] Emilien Dupont, Hrushikesh Loya, Milad Alizadeh, Adam Golinski, Y Whye Teh, and Arnaud Doucet. Coin++: Neural compression across modalities. *Transactions on Machine Learning Research*, 2022(11), 2022. [2](#), [7](#), [8](#), [9](#), [15](#)
- [12] Jonathan Richard Schwarz and Yee Whye Teh. Meta-learning sparse compression networks. *Transactions on Machine Learning Research*, 2022. ISSN 2835-8856. [1](#), [2](#), [7](#), [8](#), [15](#)
- [13] Kenneth O Stanley. Compositional pattern producing networks: A novel abstraction of development. *Genetic programming and evolvable machines*, 8(2):131–162, 2007. [2](#), [3](#)
- [14] David Minnen and Saurabh Singh. Channel-wise autoregressive entropy models for learned image compression. In *2020 IEEE International Conference on Image Processing (ICIP)*, pages 3339–3343. IEEE, 2020. [2](#), [6](#)
- [15] Dailan He, Yaoyan Zheng, Baocheng Sun, Yan Wang, and Hongwei Qin. Checkerboard context model for efficient learned image compression. In *Proceedings of the IEEE/CVF Conference on Computer Vision and Pattern Recognition*, pages 14771–14780, 2021.
- [16] Zongyu Guo, Zhizheng Zhang, Runsen Feng, and Zhibo Chen. Causal contextual prediction for learned image compression. *IEEE Transactions on Circuits and Systems for Video Technology*, 32(4):2329–2341, 2021. [6](#)
- [17] Ahmet Burakhan Koyuncu, Han Gao, Atanas Boev, Georgii Gaikov, Elena Alshina, and Eckehard G. Steinbach. Contextformer: A transformer with spatio-channel attention for context modeling in learned image compression. In *Computer Vision—ECCV 2022: 17th European Conference, Tel Aviv, Israel, October 23–27, 2022, Proceedings, Part XIX*, pages 447–463. Springer, 2022. [2](#), [6](#)
- [18] Marton Havasi, Jasper Snoek, Dustin Tran, Jonathan Gordon, and José Miguel Hernández-Lobato. Refining the variational posterior through iterative optimization, 2020. URL <https://openreview.net/forum?id=rkglZyHtvH>. [2](#), [5](#)
- [19] Gergely Flamich, Marton Havasi, and José Miguel Hernández-Lobato. Compressing images by encoding their latent representations with relative entropy coding. In *Advances in Neural Information Processing Systems*, volume 33, pages 16131–16141, 2020. [6](#)
- [20] Gergely Flamich, Stratis Markou, and José Miguel Hernández-Lobato. Fast relative entropy coding with a\* coding. In *International Conference on Machine Learning*, pages 6548–6577. PMLR, 2022. [2](#), [3](#), [4](#), [14](#)
- [21] Charles Blundell, Julien Cornebise, Koray Kavukcuoglu, and Daan Wierstra. Weight uncertainty in neural network. In *International conference on machine learning*, pages 1613–1622. PMLR, 2015. [2](#), [3](#)
- [22] Johannes Ballé, Valero Laparra, and Eero P. Simoncelli. End-to-end optimized image compression. In *5th International Conference on Learning Representations, ICLR 2017*, 2017. [2](#), [6](#)
- [23] Marton Havasi, Robert Peharz, and José Miguel Hernández-Lobato. Minimal random code learning: Getting bits back from compressed model parameters. In *7th International Conference on Learning Representations, ICLR 2019*, 2019. [2](#), [3](#), [4](#), [5](#), [6](#), [9](#), [16](#)
- [24] Alex Krizhevsky, Vinod Nair, and Geoffrey Hinton. Cifar-10 (canadian institute for advanced research). URL <http://www.cs.toronto.edu/~kriz/cifar.html>. [2](#), [7](#)
- [25] Eastman Kodak. Kodak Lossless True Color Image Suite (PhotoCD PCD0992). <http://r0k.us/graphics/kodak/>, 1993. [2](#), [7](#)
- [26] Vassil Panayotov, Guoguo Chen, Daniel Povey, and Sanjeev Khudanpur. Librispeech: An ASR corpus based on public domain audio books. In *ICASSP*, pages 5206–5210. IEEE, 2015. [2](#), [9](#), [17](#)
- [27] Chelsea Finn, Pieter Abbeel, and Sergey Levine. Model-agnostic meta-learning for fast adaptation of deep networks. In *International Conference on Machine Learning*, pages 1126–1135. PMLR, 2017. [2](#), [7](#)
- [28] George Cybenko. Approximation by superpositions of a sigmoidal function. *Mathematics of control, signals and systems*, 2(4):303–314, 1989. [3](#)
- [29] Geoffrey E Hinton and Drew Van Camp. Keeping the neural networks simple by minimizing the description length of the weights. In *Proceedings of the sixth annual conference on Computational learning theory*, pages 5–13, 1993. [3](#)

- [30] Chris J. Maddison, Daniel Tarlow, and Tom Minka. A\* sampling. In *Advances in Neural Information Processing Systems*, volume 27, pages 3086–3094, 2014. 3
- [31] Il’ya Meerovich Sobol’. On the distribution of points in a cube and the approximate evaluation of integrals. *Zhurnal Vychislitel’noi Matematiki i Matematicheskoi Fiziki*, 7(4):784–802, 1967. 3
- [32] George Papandreou and Alan L Yuille. Perturb-and-map random fields: Using discrete optimization to learn and sample from energy models. In *2011 International Conference on Computer Vision*, pages 193–200. IEEE, 2011. 3
- [33] Lucas Theis and Noureldin A. Yosri. Algorithms for the communication of samples. In *International Conference on Machine Learning*, pages 21308–21328. PMLR, 2022. 3
- [34] Durk P Kingma, Tim Salimans, and Max Welling. Variational dropout and the local reparameterization trick. In *Advances in Neural Information Processing Systems*, volume 28, 2015. 4
- [35] Diederik P. Kingma, Tim Salimans, and Max Welling. In *Variational Dropout and the Local Reparameterization Trick*, volume 28, 2015. 4, 16
- [36] Silvano Martello and Paolo Toth. Bin-packing problem. *Knapsack problems: Algorithms and computer implementations*, pages 221–245, 1990. 6
- [37] David S Johnson. *Near-optimal bin packing algorithms*. PhD thesis, Massachusetts Institute of Technology, 1973. 6
- [38] Guo Lu, Wanli Ouyang, Dong Xu, Xiaoyun Zhang, Chunlei Cai, and Zhiyong Gao. DVC: an end-to-end deep video compression framework. In *Proceedings of the IEEE/CVF Conference on Computer Vision and Pattern Recognition*, pages 11006–11015, 2019. 6
- [39] Yun He, Xinlin Ren, Danhang Tang, Yinda Zhang, Xiangyang Xue, and Yanwei Fu. Density-preserving deep point cloud compression. In *Proceedings of the IEEE/CVF Conference on Computer Vision and Pattern Recognition*, pages 2333–2342, 2022. 6
- [40] Zongyu Guo, Zhizheng Zhang, Runsen Feng, and Zhibo Chen. Soft then hard: Rethinking the quantization in neural image compression. In *International Conference on Machine Learning*, pages 3920–3929. PMLR, 2021. 6
- [41] Eirikur Agustsson and Lucas Theis. Universally quantized neural compression. In *Advances in Neural Information Processing Systems*, volume 33, pages 12367–12376, 2020. 6
- [42] L. Theis and E. Agustsson. On the advantages of stochastic encoders. In *Neural Compression Workshop at ICLR*, 2021. URL <https://arxiv.org/abs/2102.09270>. 6, 14
- [43] Lucas Theis, Tim Salimans, Matthew D. Hoffman, and Fabian Mentzer. Lossy compression with gaussian diffusion. *arXiv preprint arXiv:2206.08889*, 2022. 6
- [44] A. Shah, W.-N. Chen, J. Balle, P. Kairouz, and L. Theis. Optimal compression of locally differentially private mechanisms. In *Artificial Intelligence and Statistics*, 2022. URL <https://arxiv.org/abs/2111.00092>. 6
- [45] Vincent Sitzmann, Julien N. P. Martel, Alexander W. Bergman, David B. Lindell, and Gordon Wetzstein. Implicit neural representations with periodic activation functions. volume 33, pages 7462–7473, 2020. 7
- [46] Matthew Tancik, Pratul P. Srinivasan, Ben Mildenhall, Sara Fridovich-Keil, Nithin Raghavan, Utkarsh Singhal, Ravi Ramamoorthi, Jonathan T. Barron, and Ren Ng. Fourier features let networks learn high frequency functions in low dimensional domains. In *Advances in Neural Information Processing Systems*, volume 33, pages 7537–7547, 2020. 7
- [47] Ben Mildenhall, Pratul P. Srinivasan, Matthew Tancik, Jonathan T. Barron, Ravi Ramamoorthi, and Ren Ng. Nerf: Representing scenes as neural radiance fields for view synthesis. volume 65, pages 99–106. ACM New York, NY, USA, 2021. 7
- [48] Yannick Strömpler, Janis Postels, Ren Yang, Luc Van Gool, and Federico Tombari. Implicit neural representations for image compression. In *ECCV (26)*, volume 13686 of *Lecture Notes in Computer Science*, pages 74–91. Springer, 2022. 7
- [49] Hao Chen, Bo He, Hanyu Wang, Yixuan Ren, Ser-Nam Lim, and Abhinav Shrivastava. Nerv: Neural representations for videos. In *Advances in Neural Information Processing Systems*, volume 34, pages 21557–21568, 2021. 7

- [50] Thomas Bird, Johannes Ballé, Saurabh Singh, and Philip A. Chou. 3d scene compression through entropy penalized neural representation functions. In *2021 Picture Coding Symposium (PCS)*, pages 1–5. IEEE, 2021. 7
- [51] Matthew Tancik, Ben Mildenhall, Terrance Wang, Divi Schmidt, Pratul P. Srinivasan, Jonathan T. Barron, and Ren Ng. Learned initializations for optimizing coordinate-based neural representations. In *Proceedings of the IEEE/CVF Conference on Computer Vision and Pattern Recognition*, pages 2846–2855, 2021. 7
- [52] Jonathan Richard Schwarz, Jihoon Tack, Yee Whye Teh, Jaeho Lee, and Jinwoo Shin. Modality-agnostic variational compression of implicit neural representations. *arXiv preprint arXiv:2301.09479*, 2023. 7
- [53] 5th Workshop and Challenge on Learned Image Compression. <http://compression.cc>, 2022. 7, 16
- [54] Chelsea Finn, Kelvin Xu, and Sergey Levine. Probabilistic model-agnostic meta-learning. In *Advances in Neural Information Processing Systems*, volume 31, 2018. 10
- [55] Charles Blundell, Julien Cornebise, Koray Kavukcuoglu, and Daan Wierstra. Weight uncertainty in neural network. In *International Conference on Machine Learning*, pages 1613–1622. PMLR, 2015. 10, 17

## A Relative Entropy Coding with A\* Coding

---

### Algorithm 2 A\* encoding

---

**Require:** Proposal distribution  $p_{\mathbf{w}}$  and target distribution  $q_{\mathbf{w}}$ .

**Initialize :**  $N, G_0, \mathbf{w}^*, N^*, L \leftarrow 2^{\lceil C \rceil}, \infty, \perp, \perp, -\infty$

**for**  $i = 1, \dots, N$  **do**  $\triangleright N$  samples from proposal distribution

$\mathbf{w}_i \sim p_{\mathbf{w}}$

$G_i \sim \text{TruncGumbel}(G_{i-1})$

$L_i \leftarrow G_i + \log(q_{\mathbf{w}}(\mathbf{w}_i)/p_{\mathbf{w}}(\mathbf{w}_i))$   $\triangleright$  Perturbed importance weight

**if**  $L_i \leq L$  **then**

$L \leftarrow L_i$

$\mathbf{w}^*, N^* \leftarrow \mathbf{w}_i, i$

**end if**

**end for**

**return**  $\mathbf{w}^*, N^*$   $\triangleright$  Transmit the index  $N^*$

---



---

### Algorithm 3 A\* decoding

---

**Simulate**  $\{\mathbf{w}_i\} = \{\mathbf{w}_1, \dots, \mathbf{w}_N\}$   $\triangleright$  Simulate  $N$  samples from  $p_{\mathbf{w}}$  with the shared seed

**Receive**  $N^*$

**return**  $\mathbf{w}^* \leftarrow \mathbf{w}_{N^*}$   $\triangleright$  Receive the approximate posterior sample

---

Recall that we would like to communicate a sample from the variational posterior distribution  $q_{\mathbf{w}}$  using the proposal distribution  $p_{\mathbf{w}}$ . In our experiments, we used *global-bound depth-limited A\* coding* to achieve this [20]. We describe the encoding procedure in Algorithm 2 and the decoding procedure in Algorithm 3. For brevity, we refer to this particular variant of the algorithm as *A\* coding* for the rest of the appendix.

A\* coding is an importance sampler that draws  $N$  samples  $\mathbf{w}_1, \dots, \mathbf{w}_N \sim p_{\mathbf{w}}$  from the proposal distribution  $p_{\mathbf{w}}$ , where  $N$  is a parameter we pick. Then, it computes the importance weights  $r(\mathbf{w}_n) = q_{\mathbf{w}}(\mathbf{w}_n)/p_{\mathbf{w}}(\mathbf{w}_n)$ , and sequentially perturbs them with truncated Gumbel<sup>3</sup> noise:

$$\tilde{r}_n = r(\mathbf{w}_n) + G_n, \quad G_n \sim \text{TruncGumbel}(G_{n-1}), \quad G_0 = \infty \quad (9)$$

Then, it can be shown that by setting

$$N^* = \arg \max_{n \in [1:N]} \tilde{r}_n, \quad (10)$$

we have that  $\mathbf{w}_{N^*} \sim \tilde{q}_{\mathbf{w}}$  is approximately distributed according to the target, i.e.  $\tilde{q}_{\mathbf{w}} \approx q_{\mathbf{w}}$ . More precisely, we have the following result:

**Lemma A.1** (Bound on the total variation between  $\tilde{q}_{\mathbf{w}}$  and  $q_{\mathbf{w}}$  (Lemma D.1 in [42])). *Let us set the number of proposal samples simulated by Algorithm 2 to  $N = 2^{D_{\text{KL}}[q_{\mathbf{w}}\|p_{\mathbf{w}}]+t}$  for some parameter  $t \geq 0$ . Let  $\tilde{q}_{\mathbf{w}}$  denote the approximate distribution of the algorithm's output for this choice of  $N$ . Then,*

$$D_{\text{TV}}(q_{\mathbf{w}}, \tilde{q}_{\mathbf{w}}) \leq 4\epsilon, \quad (11)$$

where

$$\epsilon = \left( 2^{-t/4} + 2\sqrt{\mathbb{P}_{Z \sim q_{\mathbf{w}}}[\log_2 r(Z) \geq D_{\text{KL}}[Q\|P] + t]} \right)^{1/2}. \quad (12)$$

This result essentially tells us that we should draw at least around  $2^{D_{\text{KL}}[q_{\mathbf{w}}\|p_{\mathbf{w}}]}$  samples to ensure low sample bias, and beyond this, the bias decreases exponentially quickly as  $t \rightarrow \infty$ . However,

---

<sup>3</sup>The PDF of a standard Gumbel random variable truncated to  $(-\infty, b)$  is given by  $\text{TruncGumbel}(x | b) = \mathbf{1}[x \leq b] \cdot \exp(-x - \exp(-x) + \exp(-b))$ .

note that the number of samples we need also increases exponentially quickly with  $t$ . In practice, we observed that when  $D_{\text{KL}}[q_{\mathbf{w}}\|p_{\mathbf{w}}]$  is sufficiently large (around 16-20 bits), setting  $t = 0$  already gave good results. To encode  $N^*$ , we built an empirical distribution over indices using our training datasets and used it for entropy coding to find the optimal variable-length code for the index.

In short, on the encoder side,  $N$  random samples are obtained from the proposal distribution  $p_{\mathbf{w}}$ . Then we select the sample  $\mathbf{w}_i$  and transmit its index  $N^*$  that has the greatest perturbed importance weight. On the decoder side, those  $N$  random samples can be simulated with the same seed held by the encoder. The decoder only needs to find the sample with the index  $N^*$ . Therefore, the decoding process of our method is very fast. We also provide the specific coding time in Appendix E.1.

## B Closed-Form Solution for Updating Model Prior

In this section, we derive the analytic expressions for the prior parameter updates in our iterative prior learning procedure when both the prior and the posterior are Gaussian distributions. Given a set of training data  $\{\mathcal{D}_i\} = \{\mathcal{D}_1, \mathcal{D}_2, \dots, \mathcal{D}_M\}$ , we fit a variational distribution  $q_{\mathbf{w}}^{(i)}$  to represent each of the  $\mathcal{D}_i$ s. To do this, we minimize the loss (abbreviated as  $\mathcal{L}$  later)

$$\bar{\mathcal{L}}_{\beta}(\boldsymbol{\theta}_p, \{q_{\mathbf{w}}^{(i)}\}) = \frac{1}{M} \sum_{i=1}^M \mathcal{L}_{\beta}(\mathcal{D}_i, q_{\mathbf{w}}^{(i)}, p_{\mathbf{w}; \boldsymbol{\theta}_p}) \quad (13)$$

$$= \frac{1}{M} \sum_{i=1}^M \left\{ \sum_{(\mathbf{x}, \mathbf{y}) \in \mathcal{D}} \mathbb{E}_{\mathbf{w} \sim q_{\mathbf{w}}} [\Delta(\mathbf{y}, f(\mathbf{x} | \mathbf{w}))] + \beta \cdot D_{\text{KL}}[q_{\mathbf{w}}\|p_{\mathbf{w}; \boldsymbol{\theta}_p}] \right\}. \quad (14)$$

Now calculate the derivative w.r.t. the prior distribution parameter  $p_{\mathbf{w}; \boldsymbol{\theta}_p}$ ,

$$\frac{\partial \mathcal{L}}{\partial \boldsymbol{\theta}_p} = \frac{1}{M} \sum_{i=1}^M \frac{\partial D_{\text{KL}}[q_{\mathbf{w}}\|p_{\mathbf{w}; \boldsymbol{\theta}_p}]}{\partial \boldsymbol{\theta}_p} \quad (15)$$

Considering we choose factorized Gaussian as variational distributions, the KL divergence is

$$D_{\text{KL}}[q_{\mathbf{w}}^{(i)}\|p_{\mathbf{w}; \boldsymbol{\theta}_p}] = D_{\text{KL}}[\mathcal{N}(\boldsymbol{\mu}_i, \text{diag}(\boldsymbol{\sigma}_i))\|\mathcal{N}(\boldsymbol{\mu}_i, \text{diag}(\boldsymbol{\sigma}_i))] \quad (16)$$

$$= \frac{1}{2} \log \frac{\boldsymbol{\sigma}_p}{\boldsymbol{\sigma}_q^{(i)}} + \frac{\boldsymbol{\sigma}_q^{(i)} + (\boldsymbol{\mu}_q^{(i)} - \boldsymbol{\mu}_p)^2}{\boldsymbol{\sigma}_p} - \frac{1}{2} \quad (17)$$

To compute the analytical solution, let

$$\frac{\partial \mathcal{L}}{\partial \boldsymbol{\theta}_p} = \frac{1}{M} \sum_{i=1}^M \frac{\partial D_{\text{KL}}[q_{\mathbf{w}}\|p_{\mathbf{w}; \boldsymbol{\theta}_p}]}{\partial \boldsymbol{\theta}_p} = 0. \quad (18)$$

Note here  $\boldsymbol{\sigma}$  refers to variance rather than standard deviation. The above equation is equivalent to

$$\begin{aligned} \frac{\partial \mathcal{L}}{\partial \boldsymbol{\mu}_p} &= \sum_{i=1}^M \frac{\boldsymbol{\mu}_p - \boldsymbol{\mu}_q^{(i)}}{\boldsymbol{\sigma}_p} = 0, \\ \frac{\partial \mathcal{L}}{\partial \boldsymbol{\sigma}_p} &= \sum_{i=1}^M \left[ \frac{1}{\boldsymbol{\sigma}_p} - \frac{\boldsymbol{\sigma}_q^{(i)} + (\boldsymbol{\mu}_q^{(i)} - \boldsymbol{\mu}_p)^2}{\boldsymbol{\sigma}_p^2} \right] = 0. \end{aligned} \quad (19)$$

We finally can solve these equations and get

$$\boldsymbol{\mu}_p = \frac{1}{M} \sum_{i=1}^M \boldsymbol{\mu}_q^{(i)}, \quad \boldsymbol{\sigma}_p = \frac{1}{M} \sum_{i=1}^M [\boldsymbol{\sigma}_q^{(i)} + (\boldsymbol{\mu}_q^{(i)} - \boldsymbol{\mu}_p)^2] \quad (20)$$

as the result of Equation (5) in our main text. In short, this closed-form solution provides an efficient way to update the model prior from a bunch of variational posteriors. It makes our method simple in practice, unlike some previous methods [11, 12] that require expensive meta-learning loops.

## C Dynamic Adjustment of $\beta$

When learning the model prior, the value of  $\beta$  that controlling the rate-distortion trade-off is defined in advance to train the model prior at a specific bitrate point. After obtaining the model prior, we will first partition the network parameters into  $K$  groups  $\mathbf{w}_{1:K} = \{\mathbf{w}_1, \dots, \mathbf{w}_K\}$  according to the average approximate coding cost of training data, as described in Section 3.3 of the main text. Now for training the variational posterior for a given test datum, to ensure the coding cost of each group is close to  $\kappa = 16$  bits, we adjust the value of  $\beta$  dynamically when optimizing the posteriors. The detailed algorithm is illustrated here in Algorithm 4.

---

**Algorithm 4** Dynamic  $\beta$  adjustment for optimizing the posteriors

---

**Require:**  $\beta, \mathbf{w}_{1:K} = \{\mathbf{w}_1, \dots, \mathbf{w}_K\}$   
**Initialize:**  $\lambda_k = \beta, k = 1, \dots, K$   
**Initialize:** variational posterior  $q_{\mathbf{w}_k}, k = 1, \dots, K$

**for**  $i \leftarrow \text{NumberIter}$  **do**  
     $\delta_k = D_{\text{KL}}[q_{\mathbf{w}_k} \| p_{\mathbf{w}_k}], k = 1, \dots, K$   
     $q_{\mathbf{w}_{1:K}} \leftarrow \text{VariationalUpdate}(\mathcal{L}_{\lambda_{1:K}}) \quad \triangleright \mathcal{L}_{\lambda_{1:K}}$  is defined in Equation 8 in the main text  
    **if**  $(i \bmod 15) = 0$  **then**  
        **if**  $\delta_k > \kappa$  **then**  $\lambda_k = \lambda_k \cdot 1.05$   
        **end if**  
        **if**  $\delta_k < \kappa - 0.4$  **then**  $\lambda_k = \lambda_k / 1.05$   
        **end if**  
    **end if**  
**end for**  
**return**  $q_{\mathbf{w}_k}, \lambda_k, k = 1, \dots, K$

---

The algorithm is improved from Havasi et al. [23] to stabilize training, in the way that we set an interval  $[\kappa - 0.4, \kappa]$  as buffer area where we do not change the value of  $\lambda_k$ . Here we only adjust  $\lambda_k$  every 15 iterations to avoid frequent changes at the initial training stage.

## D Experiment Details

We introduce the experimental settings here and summarize the settings in Table 1.

### D.1 CIFAR-10

We use a 4-layer MLP with 16 hidden units and 32 Fourier embeddings for the CIFAR-10 dataset. The model prior is trained with 128 epochs to ensure convergence. Here, the term “epoch” is used to refer to optimizing the posteriors and updating the prior in the Algorithm 1 in the main text. For each epoch, the posteriors of all 2048 training data are optimized for 100 iterations using the local reparameterization trick [35], except the first epoch that contains 250 iterations. We use the Adam optimizer with learning rate 0.0002. The posterior variances are initialized as  $9 \times 10^{-6}$ .

After obtaining the model prior, given a specific test CIFAR-10 image to be compressed, the posterior of this image is optimized for 25000 iterations, with the same optimizer. When we finally progressively compress and finetune the posterior, the posteriors of the uncompressed parameter groups are finetuned for 15 iterations with the same optimizer once a previous group is compressed.

### D.2 Kodak

For Kodak dataset, since training on high-resolution image takes much longer time, the model prior is learned using fewer training data, i.e., only 512 cropped CLIC images [53]. We also reduce the learning rate of the Adam optimizer to 0.0001 to stabilize training. In each epoch, the posterior of

	CIFAR-10	Kodak		LibriSpeech
		Smaller Model	Larger Model	
Network Structure				
number of MLP layer	4	6	7	6
hidden unit	16	48	56	48
Fourier embedding	32	64	96	64
number of parameters	1123	12675	21563	12675
Learning Model Prior from Training Data				
number of training data	2048	512	512	1024
epoch number	128	96	96	128
learning rate	0.0002	0.0001	0.0001	0.0002
iteration / epoch (except the first epoch)	100	200	200	100
iteration number in the first epoch	250	500	500	250
initialization of posterior variance	$9 \times 10^{-6}$	$4 \times 10^{-6}$	$4 \times 10^{-6}, 4 \times 10^{-10}$	$4 \times 10^{-9}$
$\beta$	$2 \times 10^{-5}, 5 \times 10^{-6}, 2 \times 10^{-6}$ $1 \times 10^{-6}, 5 \times 10^{-7}$	$10^{-7}, 10^{-8}, 4 \times 10^{-8}$	$4 \times 10^{-6}$	$10^{-7}, 3 \times 10^{-8}$ $10^{-8}, 10^{-9}$
Optimize the Posterior of a Test Datum				
iteration number	25000	25000	25000	25000
learning rate	0.0002	0.0001	0.0001	0.0002
training with 1/4 the points (pixels)	$\times$	$\checkmark$	$\checkmark$	$\times$
number of group (KL budget = 16 bits / group)	(58, 89, 146, 224, 285)	(1729, 2962, 3264)	(5503, 7176)	(1005, 2924, 4575, 6289)
bitrate, (bpp for images, Kbps for audios)	(0.91, 1.39, 2.28, 3.50, 4.45)	(0.070, 0.110, 0.132)	(0.224, 0.293)	(5.36, 15.59, 24.40, 33.54)
PSNR, dB	(0.91, 1.39, 2.28, 3.50, 4.45)	(0.070, 0.110, 0.132)	(0.224, 0.293)	(5.36, 15.59, 24.40, 33.54)

Table 1: Hyper parameters in our experiments.

each image is trained for 200 iterations, except the first epoch that contains 500 iterations. We also reduce the total epoch number to 96 which is empirically enough to learn the model prior.

We use two models with different capacity for compressing high-resolution Kodak images. The smaller model is a 6-layer SIREN with 48 hidden units and 64 Fourier embeddings. This model is used to get the three low-bitrate points in Figure 2b in our main text, where the corresponding beta is set as  $\{10^{-7}, 10^{-8}, 4 \times 10^{-8}\}$ . Another larger model comprises a 7-layer MLP with 56 hidden units and 96 Fourier embeddings, which is used for evaluation at the two relatively higher bitrate points in Figure 2b in our main text. The betas of these two models have the same value  $2 \times 10^{-9}$ . We empirically adjust the variance initialization from the set  $\{4 \times 10^{-6}, 4 \times 10^{-10}\}$  and find they can affect the converged bitrate and achieve good performance. In particular, the posterior variance is initialized as  $4 \times 10^{-10}$  to reach the highest bitrate point in the rate-distortion curve. The posterior variance of other bitrate-points on Kodak dataset are all initialized as  $4 \times 10^{-6}$ .

**Important note:** It required significant empirical effort to find the optimal parameter settings we described above, hence our note in the Conclusion and Limitations section that Bayesian neural networks are inherently sensitive to initialization [55].

### D.3 LibriSpeech

We randomly crop 1024 audio samples from LibriSpeech “train-clean-100” set [26] for learning the model prior and randomly crop 24 test samples from “test-clean” set for evaluation. The model structure is the same as the small model used for compressing Kodak images. We evaluate on four bitrate points by setting  $\beta = \{10^{-7}, 3 \times 10^{-8}, 10^{-8}, 10^{-9}\}$ . There are 128 epochs, and each epoch

has 100 iterations with learning rate as 0.0002. The first epoch has 250 iterations. In addition, the posterior variance is initialized as  $4 \times 10^{-9}$ . The settings for optimizing and finetuning posterior of a test datum are the same as the experiments on Kodak dataset.

## E Supplementary Experimental Results

### E.1 Evaluation of Training and Practical Coding Time

**Training Time.** The most time-consuming part of setting up COMBINER for a data modality is running the iterative prior learning algorithm we propose in the main text. Furthermore, optimizing the variational posteriors takes up the bulk of the learning process since updating the prior parameters given the variational posteriors can be done efficiently using the formulae we derive in Appendix B. However, such posterior optimization can be done in parallel, especially given that our INRs have very few parameters. To train the model prior on the CIFAR-10 dataset, we can train the posteriors of 2048 images together in a single V100 GPU. It only takes around **20 minutes** to train for 128 epochs with almost 100 iterations per epoch. For training the model prior with 512 cropped CLIC images, due to the limit of GPU memory, we run multiple processes simultaneously on 4 GTX 1080 GPUs, where each process runs for a single image. The entire training time on CLIC dataset consumes around 30 hours. We note that the training time on CLIC dataset could be significantly reduced with additional engineering effort, which we leave for future work.

**Coding Time.** To compress a test datum, we first optimize its INR’s variational posterior for 25,000 iterations. Such optimization process should also be included as a part of encoding time, similar to COIN [10]. In addition, the progressive posterior refinement process also takes a long time. Therefore, the encoding time of our method is very long. Note that the encoding time of relative entropy coding is negligible compared with the optimization process because our model is very small, and there are not so many parameter groups. As a result, we are able to evaluate all the 10,000 images from the CIFAR-10 test set in parallel using a CPU cluster. To decode the network parameters, the decoder only needs to search for the sample according to the received index, which is very fast. The practical encoding and decoding time is shown in Table 2.

	CIFAR, bpp = 0.91	CIFAR, bpp = 4.45	Kodak, bpp = 0.070	Kodak, bpp = 0.293
encoding time	~10 minutes	~20 minutes	~2 hours	~4 hours
decoding time	0.051 second	0.075 second	0.410 second	0.542 second

Table 2: Practical encoding and decoding time of a specific image on 1080Ti GPU.

We show both the encoding and decoding time of our method on different datasets at different bitrates. In fact, the decoding time is mainly consumed for relative entropy decoding and inference of the received MLP network. Usually, if there are more parameter groups, the coding time will be longer. Therefore, decoding a Kodak image at our highest bitrate (0.293 bpp) consumes the most decoding time (0.542 second), but is still very fast.

### E.2 Number of Training Samples

Since the model prior is learned from a few training data, the number of training data may influence the quality of the learned model prior. We train the model prior with a different number of training images from the CIFAR-10 training set and evaluate the performance on 100 randomly selected test images from the CIFAR-10 test set. Surprisingly, as shown in Figure 6, we found that even merely 16 training images can help to learn a good model prior. Considering the randomness of training and testing, the performance on this test subset is almost the same when the number of training data exceeds 16. This demonstrates that the model prior is quite robust and generalizes well to test data. In our final experiments, the number of training samples is set to 2048 (on CIFAR-10 dataset) to ensure the prior converges to a good optimum.

### E.3 Compressing Audios with Small Chunks

The proposed approach does not need to compute the second-order gradient during training, which helps to learn the model prior of the entire datum. Hence, compression with a single Bayesian INR

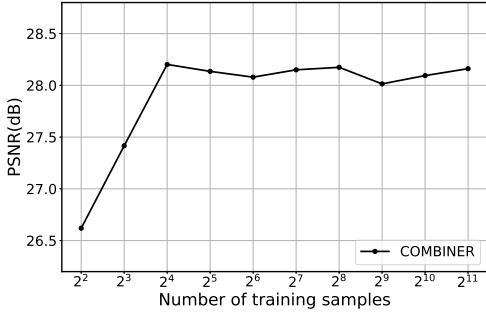


Figure 6: Impact of the number of training data.

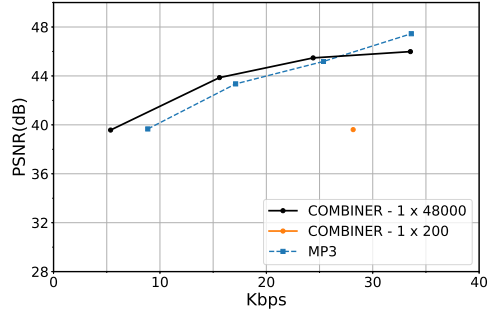


Figure 7: Compressing audios.

network helps to fully capture the global dependencies of a datum. That is the reason for our strong performance on Kodak and LibriSpeech datasets. Here, we also conduct a group of experiment to compare the influence of cropping audios into chunks. Unlike the experimental setting in our main text that compresses every 3-second audio ( $1 \times 48000$ ) with a single MLP network, here we try to crop all the 24 audios into small chunks, each of the chunk has the shape of  $1 \times 200$ . We use the same network used for compressing CIFAR-10 images for our experiments here. As shown in Figure 7, if we do not compress the audio as an entire entity, the performance will drops for around 5 dB. It demonstrates the importance of compressing with a single MLP network to capture the inherent redundancies within the entire data.

#### E.4 Additional Figures

We provide some examples of the decoded Kodak images in Figure 8.

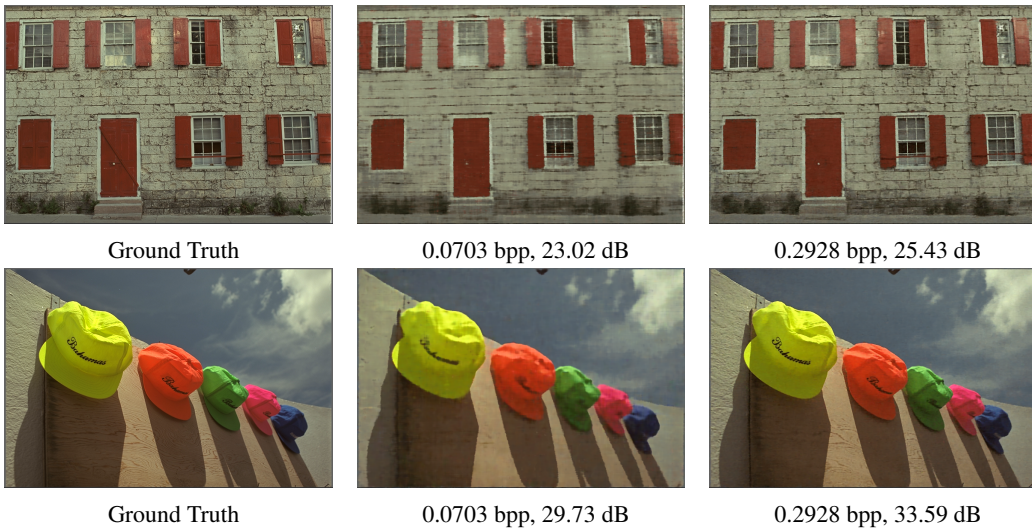


Figure 8: Decoded Kodak images.